Published in final edited form as:
J Proteome Res. 2013 June 7; 12(6): 2511–2524. doi:10.1021/pr301085c.

14-3-3ε Boosts Bleomycin-induced DNA Damage Response by Inhibiting the Drug-Resistant Activity of MVP

Siwei Tang[†,#], **Chen Bai**[‡,#], **Pengyuan Yang**[†], and **Xian Chen**[*,†,§]
Department of Chemistry and Institutes of Biomedical Sciences, Fudan University, Shanghai, China, Department of Food Science, Shanghai Business School, Shanghai, China, and Department of Biochemistry and Biophysics, University of North Carolina at Chapel Hill, Chapel Hill, North Carolina, USA

Abstract

Major vault protein (MVP) is the predominant constituent of the vault particle, the largest known ribonuclear protein complex. Although emerging evidences have been establishing the links between MVP (vault) and multidrug resistance (MDR), little is known regarding exactly how the MDR activity of MVP is modulated during cellular response to drug-induced DNA damage (DDR). Bleomycin (BLM), an anti-cancer drug, induces DNA double-stranded breaks (DSBs) and consequently triggers the cellular DDR. Due to its physiological implications in hepatocellular carcinoma (HCC) and cell fate decision, 14-3-3ε was chosen as the pathway-specific bait protein to identify the critical target(s) responsible for HCC MDR. By using LC-MS/MS-based proteomic approach, MVP was first identified in the BLM-induced 14-3-3ε interactome formed in HCC cells. Biological characterization revealed that MVP possesses specific activity to promote the resistance to the BLM-induced DDR. On the other hand, 14-3-3ε enhances BLM-induced DDR by interacting with MVP. Mechanistic investigation further revealed that 14-3-3ε, in a phosphorylation-dependent manner, binds to the phosphorylated sites at both Thr52 and Ser864 of the monomer of MVP. Consequently, the phosphorylation-dependent binding between 14-3-3ε and MVP inhibits the drug-resistant activity of MVP for an enhanced DDR to BLM treatment. Our findings provide an insight into the mechanism underlying how the BLM-induced interaction between 14-3-3ε and MVP modulates MDR, implicating novel strategy to overcome the chemotherapeutic resistance through interfering specific protein-protein interactions.

Keywords

14-3-3ε; bleomycin (BLM); major vault protein (MVP); vault; drug resistance; DNA damage response (DDR); LC-MS/MS

[*]Address correspondence to: Dr. Xian Chen, Department of Biochemistry & Biophysics, UNC School of Medicine, 120 Mason Farm Road, Genetic Medicine building, Ste 3010, CB # 7260, Chapel Hill, NC 27599-7260. xianc@email.unc.edu, Phone: 919-843-5310 Fax: 919-966-2852.
[†]Fudan University
[‡]Shanghai Business School
[§]University of North Carolina at Chapel Hill
[#]These authors contributed equally to this work

FigureS1-S4 and Table S1. This material is available free of charge via the Internet at http://pubs.acs.org.

INTRODUCTION

The development of multidrug resistance (MDR) during chemotherapeutics is the major barrier for an effective cancer therapy.[1] It is known that the altered expression of some drug transporter proteins, such as p-glycoprotein (P-gp), multidrug resistance-associated proteins (MRPs), and breast cancer resistance protein (BCRP),[2–3] are responsible for developing MDR. These transporter proteins act as ATP-dependent molecular pumps, which extrude a number of anti-cancer drugs from cells, thus decreasing their concentration around intracellular targets[1]. In addition to these drug transporter proteins, a 110kDa vesicular protein, termed lung resistance-related protein (LRP), was identified in a number of the cancer cell lines and tumors that showed intrinsic resistance to chemotherapeutic drugs.[4–7] LRP was initially found overexpressing in a non-small cell lung cancer cell line with MDR that does not express P-gp.[4] Screening of an expression library led to identification of LRP as the human form of MVP, the major component of vaults.[7] Vaults are the largest cellular ribonuclear protein complexes with the molecular weights of approximately 1.3×10^4 kDa and were characterized as the evolutionarily conserved barrel-shaped structure with a hollow interior.[8] The components composed of vault are only multiple copies of three proteins, MVP, vault poly(ADP)ribose polymerase (PARP4),[9] and telomerase-associated protein 1(TEP1).[10] One vault particle is estimated to consist of 96 molecules of MVP, 8 molecules of PARP4, 2 molecules of TEP1, and at least 6 copies of vault RNA (vRNA).[11–12] MVP only exists in vaults, which accounts for ~75% of the total mass and assembles the whole outer shell of the vault particle.[13–14] With largely unknown function, MVP(vault) is found in diverse organisms.[15] Expression of rat MVP alone in the vault-negative insect cell line can self-assemble the particles with biochemical and morphological characteristics similar to endogenous rat vaults,[13] indicating that MVP is the major determinant of the vault structure. Many evidences indicated that MVP (vault) plays a role in cellular detoxification processes and consequently contributes to MDR in cancer cell lines and tumors.[16–17] The identification of LRP as the human form of MVP implied for the first time that MVP (vault) may be involved in MDR.[7] Although drug-resistance has been correlated with the expression of MVP,[18–21] exactly how the resistance to anti-cancer drugs is acquired through MVP needs to be defined.

Hepatocellular carcinoma (HCC) is the fifth most common cancer and the third most common cause of cancer-related death worldwide.[22] The high mortality rate is mainly due to not only the unknown mechanisms of hepatocellular carcinogenesis but also the high degree of developed drug resistance in HCCs. Bleomycin (BLM), a glycopeptide drug originally isolated from *Streptomyces verticillus*,[23] has been clinically used for caner therapy.[24–25] The cytotoxic effects of BLM are associated with its nature of inducing DNA double-stranded breaks (DSBs), which is similar to those generated by ionizing radiation.[26–27] Meanwhile, based on the strength of cellular responses to BLM treatment, the cell fate-determining pathways leading to either cell survival with DNA repair or apoptosis are highly complicated and are either cell type- or genotype-dependent.[28] Chemotherapeutic drugs including BLM have been used to treat HCC.[29–31] However, due to the up-regulated expression of MDR genes (MRPs and P-gp) and lack of the understanding of drug responses in HCC cells,[32] the effectiveness of therapeutic intervention has been compromised. Thus,

the mechanistic details underlying the drug-induced DNA damage response (DDR) in HCC cells need to be revealed for developing more precise and effective strategies for HCC therapy.

The 14-3-3 proteins are abundant acidic polypeptides which are widely expressed in eukaryotes with the propensity to assemble as homo- or hetero-dimers.[33–34] Seven 14-3-3 isoforms (β, γ, ε, η, σ, θ (or τ) and ζ) have been identified in mammals. By interacting with close to 200 target proteins identified so far, these 14-3-3 isomers are known to be involved in widespread biological processes such as the regulation of cell cycle progression, the activation of MAP kinases, the initiation and maintenance of DNA damage checkpoints, the prevention of apoptosis, and the coordination of integrin signaling and cytoskeletal dynamics.[35–38] Meanwhile, proteomic screening using various 14-3-3 isoforms as the bait proteins revealed the isomer-specific composition of the interactome of different 14-3-3 family members.[39–42] The 14-3-3 epsilon (ε) isoform is the most conserved member of 14-3-3 family, with conserved sequences from plants, yeast and mammals.[33, 43] Importantly, 14-3-3ε has been implicated in regulating carcinogenesis through differential expression proteome analysis in various hepatocellular carcinoma cell lines.[44–45] Recent work found that 14-3-3ε is up-regulated in HCC, and the overexpression of 14-3-3ε is significantly associated with the high risk of tumor metastasis and poor survival,[46] all indicating that 14-3-3ε plays important roles in the carcinogenesis of HCC.

At present, the cytotoxic effects of the most chemotherapeutic drugs for cancer therapy including BLM are associated with their abilities to induce DSBs. Given the diverse roles of 14-3-3ε during HCC carcinogenesis and cell fate determination, we reason that 14-3-3ε may broadly coordinate multiple biological processes/pathways in the cellular response to BLM-induced DSBs. First, by employing LC-MS/MS-based proteomic approach, we identified/profiled the components of the 14-3-3ε interactome formed during HCC cellular response to BLM-triggered DSBs. MVP was then identified with high abundance in this phenotypic interactome, which motivated us to investigate the functional role of the interaction between MVP and 14-3-3ε during BLM-induced DDR in HCC cells given the association of MVP with MDR. Functional analyses using both siRNA-mediated gene knockdown and gene overexpression assays demonstrated that MVP indeed promotes the resistance to BLM-induced DDR while 14-3-3ε on the other hand enhances BLM-induced DDR by inhibiting MVP. Mechanistic investigation further revealed that in a phosphorylation-dependent manner 14-3-3ε binds to a monomer of MVP during HCC DDR to BLM treatment. Consequently, the phosphorylation-dependent binding of 14-3-3ε to MVP boosts the BLM-induced DDR in HCC cells by reducing the MVP-mediated drug resistance.

MATERIALS AND METHODS

Antibodies and Chemicals

FLAG antibody (200471) was purchased from Stratagene; anti-FLAG beads (A2220) was obtained from Sigma-Aldrich; MVP(sc-23917) antibody was obtained from Santa Cruz Biotech; antibodies against 14-3-3ε (ab40117), histone H3(ab32151) and γ-H2AX (ab22551) were obtained from Abcam; phospho-Chk1-S345(#2348), phospho-SPAK/JNK(Thr183/Tyr185) (#9251), Caspase-3(#9662), cleaved Caspase-3 (#9661),

PARP1(#9542) and phospho-ERK1/2(Thr202/Tyr204) (#9101) antibodies were purchased from Cell Signaling; NCL (10556-1-AP) antibody was obtained from Proteintech group Inc.; IκBα(AHO0822) antibody was purchased from Biosource; HA antibody (PA010) was obtained from Shanghai Immune Biotech.Ltd.

Sequencing-grade trypsin (V5113) was purchased from Promega; fetal bovine serum (A15-151) was purchased from PAA Laboratories; Lipofectamine 2000 (11668-019) was obtained from Invitrogen; G418 sulfate (345810) was purchased from Calbiochem; bleomycin sulfate (1076308) was purchased from United States Pharmacopeia (USP); protein G agarose (P2009) was obtained from Beyotime Institute of Biotechnology.

Plasmid Construction

Human cDNA was generated from HCC cells (QGY-7703) using a first strand cDNA synthesis kit (Takara, D6210). The Primers for N-terminal FLAG-tagged 14-3-3ε (NM_006761.4) were 5′-caccatggactacaaggacgacgatgacaaggatgatcgagaggatctggtgt-3′ and 5′-gtcagatttggtggttctcagtgac-3′. The FLAG-14-3-3ε PCR product was directly introduced into pcDNA™3.1 Directional TOPO Expression vector (Invitrogen, K4900-40) according to the manufacturer's protocol.

The primers for the HA-tagged full-length MVP (NM_017458.3), N-terminal MVP repeat domain (1-530AA, MVP-N) and the MVP C-terminal domain (521-893AA, MVP-C) were 5′-gagcgtcgaccatggcaactgaagagttcatc-3′/5′-cggcggtacctttgcccagaaacttccattg-3′, 5′-gagcgtcgaccatggcaactgaagagttcatc-3′/5′-cgcgggtaccttattcgatggtgatgacgtctg-3′ and 5′-tcgcgtcgaccgacttcttcacagacgtcat-3′/5′-cggcggtacctttgcccagaaacttccattg-3′, respectively. PCR products of these genes were introduced into pCMV-HA vector (Clontech) between SalI and KpnI sites.

The primers for HA-tagged MVP mutants, including T52A, S864A were as follows: 5′-catgcgcatggtggccgtccccccacgtcactac-3′/5′-gtagtgacgtgggggacggccaccatgcgcatg-3′ and 5′-gcagaagggtggccgctgggcccagccctg-3′/5′-cagggctgggcccagcggccacccttctgc-3′, respectively. The MVP-T52A, S864A and T52A/S864A (double-mutant, DM) mutants were then generated using site-directed mutagenesis method. All of the above insert constructs were confirmed by DNA sequencing.

Cell Culture, Selection of Stable HCC Cell Line, BLM Treatment and Protein Extraction

QSG-7701(hepatocyte) and QGY-7703(hepatocellular carcinoma) cell lines were purchased from the Cell Bank of Chinese Academy of Science (Shanghai, China) and grown in RPMI 1640 medium supplemented with 10% FBS;[47] HEK-293T[48] and Hela cell lines[49] were maintained in high glucose DMEM medium supplemented with 10% FBS.

Stable FLAG-tagged 14-3-3ε expressing HCC cells were obtained by screening transfected HCC cells with 400μg/ml G418.

Cells were treated with or without BLM, and the whole cell lysate (WCL) was extracted with lysis buffer (Beyotime P0013) supplemented with protease inhibitor cocktail (Sigma-Aldrich, P8340) and phosphatase inhibitor cocktail (Sigma--Aldrich, P5726).

Histone extraction was performed using a method similar to the previously described with some modifications.[50] Briefly, cells treated with or without BLM were lysed in lysis buffer (0.5% NP40, 100 mM NaCl, 50 mM Tris, 1 mM EDTA, protease inhibitor cocktail (Sigma-Aldrich, P8340) and phosphatase inhibitor cocktail (Sigma-Aldrich, P5726)). After centrifugation, the supernatants were kept as cytoplasmic fractions. Histones were extracted by resuspending the pellets with 0.2M HCl overnight at 4°C. The HCl extracts were centrifuged, and the supernatants (histone extracts) were then neutralized with NaOH and blotted with anti-γ-H2AX or histone H3 antibody.

Purification of BLM-induced 14-3-3ε Interacting Complex, Protein Digestion and Peptide Extraction

Approximately 1×10^9 stable FLAG-14-3-3ε expressing HCC cells treated with 20mU/ml BLM for 2h were lysed with lysis buffer (Beyotime, P0013) supplemented with protease inhibitor cocktail (Sigma-Aldrich, P8340) and phosphatase inhibitor cocktail (Sigma-Aldrich, P5726). The supernatants were incubated with 300μl anti-FLAG beads (Sigma-Aldrich, A2220) at 4°C for 4h on a gentle rotating device. After immunoprecipitation, anti-FLAG beads were washed for five times with TBS buffer (50 mM Tris-HCl, pH7.4, 150 mM NaCl) to eliminate non-specific binding. Immunoprecipitates were then eluted by 100μg/ml of 1×FLAG peptide (Sigma). Eluates were concentrated to the appropriate volume for the following SDS-PAGE separation and Coomassie Blue staining. The visible bands cutting, in-gel trypsin digestion, and peptides extraction were performed following the previously described protocol.[51]

LC-MS/MS Analysis

LC-MS/MS experiments were performed on a hybrid linear quadruple ion trap/Orbitrap (LTQ-Orbitrap) mass spectrometer (Thermo Finnigan, Bremen, Germany) coupled to a Shimadzu LC-20AD LC system (Shimadzu, Japan) and SIL-20AC autosampler (Shimadzu, Japan). Peptide mixtures were separated using a PICOFRIT C18 reverse-phase column (0.075×100 mm, New Objective Inc., Woburn, MA) with a 110 min-gradient at a flow rate of 300 nL/min. Samples were loaded in solvent A (95% H_2O, 5% ACN, 0.1% formic acid), and peptides were eluted by 5% solvent B (5% H_2O, 95% ACN, 0.1% formic acid) for 5 min followed by a linear gradient to 45% solvent B in the next 90 min, ramping up to 95% solvent B in 4 min and dropping to 90% solvent B for 4 min before re-equilibrating the system to 10% solvent B for 7 min. The LTQ-Orbitrap mass spectrometry was operated in the data-dependent mode using the TOP3 strategy. Briefly, a scan cycle was initiated with a full scan of mass range (*m*/*z* 400–2000) in the Orbitrap under the target mass resolution of 100 000, which was followed by MS/MS scans in the linear ion trap on the three most abundant precursor ions. The single-charged ions were excluded from MS/MS analysis. Spectra were acquired under automatic gain control (AGC) for survey spectra (AGC: 10^6) and for MS/MS spectra (AGC: 10^4). The spray voltage was 1.6 kV and the temperature of ion transfer capillary was 180°C.

Database Search and Protein Identification

Tandem mass spectra were extracted by Bioworks Version 3.3.1 SP1 (ThermoFisher, San Jose, CA) and submitted to the human International Protein Index database (IPI human 3.45, 71983 entries) using TurboSequest V.28 (rev. 13) search engine. The search criteria were used as follows: full tryptic enzyme specificity; 2 missed cleavages; 10 ppm peptide tolerance and 0.8 Da fragment ion tolerance were allowed; dynamic modifications include phosphorylated Ser/Thr/Tyr (+79.9663) and oxidized Met (+15.9994). TurboSequest results were filtered by Xcorr, peptide probability and Delta Cn. Xcorr was set at 1.9, 2.7, 3.5 for 1+, 2+ and 3+ charged precursor ions, respectively; peptide probability<0.001, delta Cn>0.1, and keratin (most of them are contaminants) was excluded. Each protein identified requires the match of at least two peptides. The data's false positive rate was estimated to be less than 1% by reverse database search. The reverse database was generated from IPI human 3.45 (71983 entries).

Cell Transfection and RNA Interference

Transfection was carried out in 60mm dishes. Briefly, 4.0μg of HA-tagged constructs were transfected alone or co-transfected with 4.0μg FLAG-tagged 14-3-3ε into cells using Lipofectamine 2000 transfection reagent according to the manufacture's protocol. Cells were analyzed after 48h of transfection.

Scrambled siRNA (negative control) (AM4611) was purchased from Ambion, Inc. The siRNA specific to human MVP used in this study was the same as that described previously.[52] The siRNAs specific to human 14-3-3ε were designed and synthesized by Shanghai GenePharma Co., Ltd, China. The siRNA target sequences for 14-3-3ε were as follows: #1(5′-CGCUGAGUGAAGAAAGCUATT-3′,5′-UAGCUUUCUUCACUCAGCGTT-3′), #2(5′-GCUUAGGUCUUGCUCUCAATT-3′,5′-UUGAGAGCAAGACCUAAGCTT-3′) and #3(5′-GGAGGAGAAGACAAGCUAATT-3′, 5′-UUAGCUUGUCUUCUCCUCCTT-3′). The siRNAs (40nM) were transfected into cells using Lipofectamine 2000 transfection reagents. Cells were analyzed after 48h of transfection.

Gel Filtration Analysis

HEK-293T cells in two 100mm dishes were co-transfected with 12μg of HA-MVP plasmid and 12μg of FLAG-14-3-3ε plasmid using Lipofectamine 2000 transfection reagent. 40h after transfection, cells were treated with BLM (20mU/ml, 2h) and lysed with lysis buffer (20mM Tris-HCl pH7.6, 150mM NaCl, 0.3% NP-40 supplemented with protease inhibitor cocktail (Sigma-Aldrich, P8340) and phosphatase inhibitor cocktail (Sigma-Aldrich, P5726)). After centrifuge, the cell extracts were prepared for the following gel filtration analysis.

Gel filtration analysis was performed with ÄKTApurifier system (GE Healthcare) on a Superose 6 10/300 GL column (GE Healthcare) equilibrated with PBS buffer. The exclusion limit of column is 4×10^4kDa, and an optimal separation range from 5000 to 5×10^3kDa. 1.4ml of 293T cell extracts prepared as above was loaded on the column and eluted at a flow rate of 0.5ml/min. The eluted fractions (0.5ml/fraction) both in high molecule weight area

(B12 to C3 fractions) and low molecule weight area were combined (C4 to C12 fractions), respectively (shown in Figure 4A). The two combined fractions were concentrated to 1.5ml by ultrafiltration (Millipore, UFC901008) and were incubated with anti-FLAG beads for immunoprecipitation, respectively. Before the combination of fractions for immunoprecipitation, some fractions (100μl each) collected in high and low molecule weight areas respectively were analyzed by immunoblotting to check the distribution of MVP and 14-3-3ε proteins.

Co-immunoprecipitation and Immuoblotting

The procedure used for protein isolation and immunoprecipitation with anti-FLAG beads was essentially the same as that described in purification of 14-3-3ε interacting complex for MS identification except that the immunoprecipitates were eluted by directly boiling the beads.

To immunoprecipitate 14-3-3ε using an MVP antibody, QGY-7703 cells ($1–2\times10^7$ cells/assay) treated with or without BLM were lysed and 2μg of mouse monoclonal MVP antibody (Santa Cruz, sc-23917) were then added into the solution fractions of each group and incubated at 4°C overnight with gentle shaking. On the following day, 40μl of agarose-conjugated protein G was added into each group and incubated at 4°C for 4h with gentle shaking. After incubation, the immunoprecipitates were washed for five times with PBS to eliminate non-specific binding. Immunoprecipitates were eluted by directly boiling the beads.

Samples were separated on appropriate concentration of SDS-PAGE gel and transferred onto PVDF membranes (Immobilon-PSQ Membrane, 0.2_m). The membranes were blocked with TBST containing 5% non-fat milk and incubated with the specified primary antibody at room temperature for 1–2h or overnight at 4°C with gentle shaking followed by incubation with secondary antibody conjugated with horseradish peroxidase. Finally, ECL substrate was added to the membrane and exposed using the ECL system.

RESULTS

MVP Promotes the Resistance in the Cellular Response of HCC to BLM-Induced DSBs

We first established a HCC cell line that stably expresses a functional FLAG-tagged 14-3-3ε and examined the dose- and time-dependent responses of the HCC stable cells to BLM treatment (Supporting Information, Figure S1). We observed that BLM triggers the apoptosis in the HCC cells stably expressing FLAG-14-3-3ε in both dose- and time-dependent manner. Indicated by multiple apoptotic markers including the cleavage of Caspase 3,[53–54] and the release of its substrate PARP1,[55] a treatment with a high-dose BLM (150mU/ml) for 4 hours showed higher degree of apoptosis in the stable HCC cells than that induced by a lower dose (20mU/ml) and a shorter time (2 hours) (Supporting Information, Figure S1B-D). Further, comparative analyses of BLM-induced, dose- and time-dependent DDR indicated the followings (Supporting Information, Figure S1C-D): The levels of both phospho-serine 139 H2AX or γ-H2AX, and phosphorylated Chk1(pS345), the commonly used DSB markers,[56–57] were increased in the BLM dose- and time-dependent manner.

Additionally, several MAPKs, such as ERK1/2 and SPAK/JNK (p54/p46) as well as MAPK-dependent IκB-α degradation were all induced by BLM in the similar manner. Given the observation of a large population of apoptotic cells found with the high-dose BLM stimulation (150mU/ml, 4h), we chose the condition in which stable HCC cells were treated with 20mU/ml BLM for 2h for proteomic profiling the BLM-induced, HCC-specific 14-3-3ε interactome. Following the BLM treatment and immunoprecipitation using anti-FLAG beads, the immunoprecipitates were subjected to SDS-PAGE separation, in-gel trypsin digestion, and LC-MS/MS identification (Supporting Information, Figure S2). MVP was then identified with high confidence in the 14-3-3ε interactome formed in the stable HCC cells treated by BLM along with PARP4 and TEP1, the other two minor vault components (Table 1, Supporting Information, Table S1).

Given that MVP is known as a highly abundant protein expressed in a variety of tissues and cells,[15, 58] firstly, we comparatively examined the level of MVP expression in four different types of human cell lines, including QGY-7703 (HCC cells), QSG-7701 (hepatocytes), HEK-293T (human embryonic kidney cells) and Hela (human cervical carcinoma cells), by immunoblotting using a monoclonal MVP antibody. As shown in Figure 1A, MVP expression was detected respectively in QSG-7701, QGY-7703, and Hela cells except for HEK-293T cells, suggesting that HEK-293T can be used as a MVP-depleted control cell line for studying MVP function in depth.

Secondly, we examined the cellular DDR to BLM treatment in QSG-7701, Hela, and HEK-293T cells, respectively. Cells were stimulated with 20mU/ml BLM for different time points. As shown in Figure 1B, in these cell lines, the levels of γ-H2AX, phosphorylated Chk1 and phosphorylation-dependent IκB-α degradation were all shown in a BLM-inducible and time-dependent manner similar to that observed in HCC cells (Supporting Information, Figure S1C). These findings indicated that the cellular DDR to BLM takes place in these cell lines. However, the maximum activation of ERK1/2 triggered by BLM differed among these cell lines, indicating that some MAPKs activation induced by BLM was cell type-dependent.

Based on that BLM triggers the cellular DDR in all tested cell lines as described above, we then determined whether MVP possesses the activity to resist BLM-induced DDR in these cells. Scrambled siRNA (NC-siRNA) and MVP siRNA were respectively transfected into each of three MVP-expressing cell lines including QSG-7701, QGY-7703 and Hela cells (Figure 1A). Following BLM treatment (20mU/ml, 2h) and subcelluar fractionation, indicated by γ-H2AX, we observed that the knock-down of MVP resulted in a remarkable elevation of the cellular DDR to BLM in all three MVP-expressing cell lines (Figure 2A). Furthermore, transfection of exogenous MVP into HEK-293T cells, the MVP-depleted cell line, also led to a resistance to BLM-induced DDR (Figure 2B), all clearly demonstrating that MVP indeed possesses the resistant activity to BLM-induced DDR.

14-3-3ε Enhances BLM-induced DDR by Inhibiting the BLM-resistant Activity of MVP

Through interacting with numerous phosphorylated proteins with diverse functions 14-3-3 proteins play an integral role in the core phospho-regulatory pathways/biological processes such as mitogenic and cell survival signaling, cell cycle control, and apoptotic cell death,

attributing to an oncogenic potential[59]. In HCC, 14-3-3ε isoform was found to be up-regulated in correlation with the high risk of tumor metastasis and poor survival[46], further validating the role of 14-3-3 proteins in cancer development and progression. Specifically, during DDR, 14-3-3ε directly interacts with CDC25C to inhibit cell cycle progression[60-61] as well as binds p53 to negatively regulate p21 expression, therefore inducing G1 arrest after DNA damage[62].

Given 14-3-3ε plays multiple roles in these cell fate-determining pathways involved in cell apoptosis and survival during cellular DDR, we first clarified the role of 14-3-3ε in BLM-induced DDR. As shown in Figure 2C, knocking-down 14-3-3ε led to a general decrease of BLM-induced DDR in all MVP-expressing cell lines, as evidenced by the level of γ-H2AX level, indicating that 14-3-3ε positively regulate the cellular DDR induced by BLM. Together with that MVP could reduce BLM-induced DDR (Figure 2A-B) we reasoned that 14-3-3ε may interplay with MVP during BLM-induced DDR.

We then transfected the construct expressing either HA-tagged MVP or FLAG-tagged 14-3-3ε or both into each of the three MVP-expressing cell lines, including QSG-7701, QGY-7703, and Hela (Figure 1A). Results of immunoblotting analysis indicated that in response to BLM treatment, overexpression of either MVP or 14-3-3ε alone respectively led to either a reduced or an increased DDR compared to those of control cells as indicated by the changes of γ-H2AX (Figure 2D and Supporting Information, Figure S3), consistently agreeing with the observations caused by siRNA-mediated knockdown of either MVP or 14-3-3ε, respectively (Figure 2A and 2C). Co-expression of 14-3-3ε with MVP recovered more DDR to BLM compared to that of expression of MVP alone, all indicating that 14-3-3ε promotes the DDR to BLM by negatively regulating the BLM-resistant activity of MVP.

BLM Induces Site-specific Phosphorylation of MVP that Promotes its Binding to 14-3-3ε

Next, we clarified the correlation between the association of 14-3-3ε with MVP and BLM-induced DDR, and further revealed the mechanism underlying how 14-3-3ε regulates the BLM-resistant activity of MVP. By using reciprocal immunoprecipitation, MVP was found as a BLM-induced 14-3-3ε interactor in HCC cells (Figure 3A-B), consistent with the proteomic identification of MVP in the BLM-induced HCC-specific 14-3-3ε interactome by LC-MS/MS (Table 1, Supporting Information, Table S1). We also examined how the interaction between 14-3-3ε and MVP responds to increasing doses of BLM. An elevated DDR was observed in the stable FLAG-14-3-3ε cells treated with a high-dose BLM (150mU/ml, 4h) as evidenced by multiple DDR markers (Supporting Information, Figure S1D). In the immunoprecipitates pulled-down by anti-FLAG beads, the binding between 14-3-3ε and MVP was enhanced along with the elevated DDR triggered by high-dose BLM (Figure 3C), indicating that the interaction between 14-3-3ε and MVP is BLM-inducible.

Previous studies showed that most MVP monomers are rapidly incorporated into vaults.[63-64] MVP-assembled vault particle is a dynamic structure, and the exchange between MVP monomers and vault-incorporated MVP is rather fast.[65] We therefore determined the form of MVP, either monomer or multimer when it associates with 14-3-3ε during BLM-induced DDR. Firstly, HA-tagged MVP and FLAG-tagged 14-3-3ε were co-transfected into

HEK-293T, the MVP-depleted cells. 40 hours after the transfection, cells were treated with BLM (20mU/ml, 2h) and lysed. The cell extracts were then subjected to chromatographic fractionation (Figure 4A). Analysis of gel-filtration fractions by immunoblotting demonstrated that MVP predominantly exists as multimer with a minor population of monomer (Figure 4B), which is consistent with the notion that MVP predominantly exists as multimer in cells. Furthermore, we found that 14-3-3ε was not co-eluted with the multimerized MVP (Figure 4B).

Using anti-FLAG beads we conducted immunoprecipitation experiments respectively with the fraction containing either multimerized or monomer MVP. As shown in Figure 4C, the monomers of MVP were found to be associated with 14-3-3ε, and the association is BLM-inducible. To determine which domain of MVP could mediate 14-3-3ε binding, the construct expressing FLAG-14-3-3ε was co-transfected with either of the two truncated HA-tagged constructs expressing the N-terminal repeat domain (MVP-N, 1-530AA) or the C-terminal domain (MVP-C, 521-893AA) of MVP into HCC or HEK-293T cells, respectively. Results of immunoblotting analysis of the immunoprecipitates pulled-down from BLM-stimulated versus non-stimulated cells revealed that upon BLM induction 14-3-3ε enhanced its binding primarily to MVP-N not to MVP-C which was decreased in the affinity following BLM treatment (Figure 5, A: in HEK-293T cells; B: in HCC cells).

Given that most of 14-3-3's interacting partners are the phosphorylated proteins containing the characteristic 14-3-3 binding motifs, RXXpS/TXP or RXXXpS/TXP (pS/T represents phospho-serine/threonine, X stands for any amino acid),[66] we reasoned that, based on the results of domain mapping (Figure 5), there are putative 14-3-3 binding motifs in MVP that may undergo site-specific phosphorylation upon BLM stimulation. We then scanned the MVP sequence and found two evolutionarily conserved, putative 14-3-3 binding motifs including one of R49-P54 (RMVTVP) at the MVP N-terminus, and another of R860-P866 (RRVASGP) at the C-terminus where T52 and S864 are the putative phosphorylation sites in their respective motifs (Figure 6A).

We constructed a series of HA-tagged MVP mutants including T52A, S864A, and T52A/S864A (double-mutant, DM), in which the threonine (T) or serine (S) residue was substituted by non-phosphorylatable alanine (A). Following the co-transfection of FLAG-14-3-3ε with either wild-type (WT) MVP or each of the individual mutants into the MVP-depleted HEK-293T cells, comparative immunoblotting analyses of the immunoprecipitates pulled-down by anti-FLAG beads from the transfected cells treated with BLM indicated the followings (Figure 6B and Supporting Information, Figure S4): (1) The binding of 14-3-3ε to the T52A mutant was clearly weakened with respect to that to the wild-type MVP, indicating that BLM indeed induces the phosphorylation of T52 at the N-terminal MVP to promote its 14-3-3ε binding, (2) The binding of 14-3-3ε to the S864A mutant was actually stronger than that of 14-3-3ε to the T52A mutant, but was weaker than that to wild-type MVP. The 14-3-3 binding motif containing S864 resides in MVP-C which showed a weaker binding to 14-3-3ε in the BLM-stimulated cells (Figure 5), indicating that S864 could be phosphorylated in non-stimulated cells rather than in BLM-treated cells. The dephosphorylation of phospho-S864 could happen upon BLM stimulation, leading to a decreased binding of 14-3-3ε to MVP. The substitution of serine by alanine at 864

contributes to the weakened 14-3-3ε binding of S864A mutant, (3) Unexpectedly, the double mutant, T52A/S864A (DM) showed a stronger binding to 14-3-3ε even more than that of 14-3-3ε to T52A. MVP was reported as a phosphoprotein targeted by protein kinase C *in vitro*, or by a tyrosine kinase i*n vivo*.[67–68] SHP-2 (tyrosine phosphatase) was shown to associate with tyrosyl-phosphorylated MVP via its SH2 domain.[69] Meanwhile, 14-3-3 proteins were found to constitutively associate with SHP-2 during DDR[70], as well as TEP1 along with MVP and PARP4 for assembling the vault particle.[71] T52 locates in the first anti-parallel β-strand within the MVP repeat domain, and S864 resides in the cap-ring domain of MVP C-terminus.[72] Both T52 and S864 are hydrophilic residues which are important for stabilizing the conformation of MVP. Mutation of these two sites to Ala might induce a conformational change of MVP to facilitate the phosphorylation of other sites induced by BLM, resulting in an enhancement of 14-3-3ε binding with the T52A/S864A mutant. However, the following experimental results indeed supported the hypothesis that both T52 and S864 residues on MVP were involved in mediating 14-3-3ε binding (Figure 7).

In summary, by using a combined approach including immunoprecipitation, gel filtration, and site-directed mutagenesis, we demonstrated that MVP binding to 14-3-3ε is indeed phosphorylation-dependent during BLM-induced DDR. Moreover, expression of exogenous MVP in MVP-depleted cells (HEK-293T) could result in the formation of multimerized MVP, indicating that most of MVP monomers could self-assemble as a vault-like structure or MVP monomers together with endogenous PARP4 and TEP1 in integral vault particles.

14-3-3ε via its Binding to MVP Enhances BLM-induced DDR by Inhibiting the BLM-Resistant Activity of MVP

To determine whether the 14-3-3ε-MVP interaction could directly regulate the BLM-resistant activity, we extracted the histone fractions from HEK-293T cells in which each of HA-tagged MVP mutants (WT, T52A, S864A and T52A/S864A) were individually co-transfected with FLAG-tagged 14-3-3ε to identify the 14-3-3ε binding sites on MVP (Figure 6B). Using γ-H2AX as a DDR marker, we examined the BLM-induced DDR in each co-transfected cells by immunoblotting. As shown in Figure 7A, cells transfected with the T52A/S864A and T52A mutants showed considerably less BLM-induced DDR compared to the cells transfected with wild-type MVP. Additionally, the DDR of T52A/S864A mutant-expressing cells was slightly weaker than that of T52A mutant-expressing cells. Furthermore, the cells expressing S864A mutant also showed slightly weaker DDR compared to that of wild-type MVP-expressing cells. We also transfected these MVP mutants into a MVP-expressing HCC cell line (QGY-7703). As shown in Figure 7B, the trend of cellular DDR to BLM among each individual MVP mutant-expressing cells was similar to that observed in the HEK-293T cells.

Given that T52 and/or S864 sites on MVP were found to be involved in 14-3-3ε binding in response to BLM treatment (Figure 6B), the substitution of these two sites with Ala led to the impairment of 14-3-3ε binding to MVP. Therefore, these MVP mutants were free to exert more resistance to BLM compared to that of wild-type MVP. Although the binding of 14-3-3ε to T52A/S864A mutant was stronger than that of T52A mutant to 14-3-3ε (Figure

6B), the phosphorylation changes at both sites are critical in mediating the MVP binding to 14-3-3ε.

Taken these results together, we concluded that 14-3-3ε negatively regulating the BLM-resistance activity of MVP through its phosphorylation-dependent binding to MVP.

DISCUSSION

Vaults are the largest ribonucleoprotein particles with a hollow barrel-shaped structure.[8] The components composed of vault are only multiple copies of three proteins, MVP, PARP4 and TEP1.[7, 9–10] MVP constitutes over 70% of the molecular mass of vaults and is the major determinant of the vault structure.[13] MVP (vault) was found frequently up-regulated in a variety of cancer cell lines and tumors that is intrinsically resistant to chemotherapeutic drugs,[12, 16, 19] indicating the correlation between MVP (vault) and multidrug resistance (MDR). However, the exact mechanisms underlying the regulation of MVP (vault)-mediated cellular resistance toward chemotherapeutics is largely unknown.

With their phospho-serine/phospho-threonine binding modules 14-3-3 proteins interacts with specific proteins that are involved in various phospho-dependent regulatory pathways such as cell cycle, MAPK signal transduction, DDR and apoptosis,[38, 73] as well as those involved in the regulation of various oncogenes and tumor suppressor genes.[74–75] To better understand how HCC DDR is regulated during cancer chemotherapy, we employed LC-MS/MS-based proteomic approach to profile/identify the components of the 14-3-3ε interactome formed during HCC cells in response to BLM-induced DSBs. MVP along with PARP4 and TEP1, the two minor components of vault, were identified with high confidence as the BLM-induced 14-3-3ε interacting partners (Table 1, Supporting Information, Table S1).

Given that MVP is associated with MDR, it motivated us to investigate the functional role of the interaction between MVP and 14-3-3ε during BLM-induced DDR. By using both siRNA-mediated knockdown and overexpression assays (Figure 2), we demonstrated that MVP indeed possesses the BLM-resistant activity during BLM-induced DDR. In contrast, 14-3-3ε was found to positively regulate BLM-induced cellular DDR. Mechanistically, 14-3-3ε, in a phosphorylation-dependent manner, binds to MVP monomers (at phosphorylated T52 and S864 sites) during BLM-induced DDR(Figure 3–6). As a consequence, the binding of 14-3-3ε to MVP monomer directly inhibits the drug-resistant activity of MVP to boost BLM-induced DDR in cells (Figure 7). Meanwhile MVP was reported as a highly phosphorylated protein,[67–68] S864[76] and other putative phosphorylation sites (Y13,[77–78] Y15,[79] S445,[80] T830/T833,[81] S873,[82–83] and S876[84]) were identified by phosphoproteomic analysis in various human tissues and cell lines without biological validation. We here characterized the roles of two newly identified phosphorylation sites of MVP in mediating the functional interaction between 14-3-3ε and MVP.

It has been postulated that vaults could internalize drugs into their hollow cavity and transport them to efflux pumps (P-gp, MRPs and BCRP) and exocytotic vesicles, leading to the drug departure from their intracellular targets or be out cells, consequently, reducing the

drug effectiveness.[16] MVP monomers spontaneously form the vault particles without the need for other vault components such as PARP4 and TEP,[13] indicating that MVP molecules are responsible for directing the vault particle assembly. In addition, vault particles are dynamic structure, the exchange between MVP monomers and vault-incorporated MVP is rather fast.[65] Based on this knowledge together with our observations in the present study, we propose a model illustrating how 14-3-3ε promotes BLM-induced DDR through inhibiting MVP (Figure 8). In response to BLM treatment, MVP T52 was phosphorylated, which together with the phosphorylated MVP S864 mediates the binding of the 14-3-3 dimer to MVP monomers. This binding may interfere with MVP-mediated vault assembly or inhibit the exchange between MVP monomers and vault-mounted MVP molecules, ultimately leading to a reduction of the numbers of intact functional vault particles for drug sequestration. *i.e.*, this process results in increases of BLM accumulation at their targets followed by DNA damage and elevated cellular DDR. Here, we also observed that overexpression of MVP in the MVP-absence cell line, HEK-293T, results in forming multimerized MVP as well as the resistance to BLM-induced DDR (Figure 4 and Figure 2B). These results indicate that exogenous MVP molecules can assemble as minimal vault structure or MVP molecules together with endogenous PARP4 and TEP1 assembles as integral vault particles, therefore extruding BLM away their intracellular targets and consequently decreasing BLM-induced DDR. These observations support an assumption that the drug-resistant activity of MVP is exerted dependent upon the vault-like or the integral vault structure that MVP monomer is incorporated in. The questions regarding which kinases are responsible for MVP phosphorylation, and how the interaction between 14-3-3ε and phosphorylated MVP affects vault assembly remain to be investigated.

Supplementary Material

Refer to Web version on PubMed Central for supplementary material.

Acknowledgments

This work was supported by grants from Shanghai Science and Technology Development Program (Grants 03DZ14024 and 07ZR14010) and the 863 High Technology Foundation of China (Grant 2006AA02A310). This work was also supported by the Innovation Program of Shanghai Municipal Education Commission (No. 10YZ212).This work is also supported in part by NIH grants to X.C. (NIH R01AI064806 and portions of this work were also supported by grant (1U24CA160035) from the National Cancer Institute Clinical Proteomic Tumor Analysis Consortium (CPTAC)). We thank Mr. Jun Yao for his assistance in mass spectrometry analysis.

References

1. Gottesman MM, Fojo T, Bates SE. Multidrug resistance in cancer: role of ATP-dependent transporters. Nat Rev Cancer. 2002; 2(1):48–58. [PubMed: 11902585]
2. Keppler D. Multidrug resistance proteins (MRPs, ABCCs): importance for pathophysiology and drug therapy. Handb Exp Pharmacol. 2011; (201):299–323. [PubMed: 21103974]
3. Sharom FJ. ABC multidrug transporters: structure, function and role in chemoresistance. Pharmacogenomics. 2008; 9(1):105–27. [PubMed: 18154452]
4. Scheper RJ, Broxterman HJ, Scheffer GL, Kaaijk P, Dalton WS, van Heijningen TH, van Kalken CK, Slovak ML, de Vries EG, van der Valk P. Overexpression of a M(r) 110,000 vesicular protein in non-P-glycoprotein-mediated multidrug resistance. Cancer Res. 1993; 53(7):1475–9. [PubMed: 7680954]

5. Izquierdo MA, van der Zee AG, Vermorken JB, van der Valk P, Belien JA, Giaccone G, Scheffer GL, Flens MJ, Pinedo HM, Kenemans P. Drug resistance-associated marker Lrp for prediction of response to chemotherapy and prognoses in advanced ovarian carcinoma. J Natl Cancer Inst. 1995; 87(16):1230–7. [PubMed: 7563169]
6. List AF, Spier CS, Grogan TM, Johnson C, Roe DJ, Greer JP, Wolff SN, Broxterman HJ, Scheffer GL, Scheper RJ, Dalton WS. Overexpression of the major vault transporter protein lung-resistance protein predicts treatment outcome in acute myeloid leukemia. Blood. 1996; 87(6):2464–9. [PubMed: 8630412]
7. Scheffer GL, Wijngaard PLJ, Flens MJ, Izquierdo MA, Slovak ML, Pinedo HM, Meijer C, Clevers HC, Scheper RJ. The drug resistance-related protein LRP is the human major vault protein. Nat Med. 1995; 1(6):578–582. [PubMed: 7585126]
8. Kedersha NL, Heuser JE, Chugani DC, Rome LH. Vaults. III. Vault ribonucleoprotein particles open into flower-like structures with octagonal symmetry. J Cell Biol. 1991; 112(2):225–35. [PubMed: 1988458]
9. Kickhoefer VA, Siva AC, Kedersha NL, Inman EM, Ruland C, Streuli M, Rome LH. The 193-kD vault protein, VPARP, is a novel poly(ADP-ribose) polymerase. J Cell Biol. 1999; 146(5):917–28. [PubMed: 10477748]
10. Kickhoefer VA, Stephen AG, Harrington L, Robinson MO, Rome LH. Vaults and telomerase share a common subunit, TEP1. J Biol Chem. 1999; 274(46):32712–7. [PubMed: 10551828]
11. Kong LB, Siva AC, Rome LH, Stewart PL. Structure of the vault, a ubiquitous celular component. Structure. 1999; 7(4):371–9. [PubMed: 10196123]
12. Scheffer GL, Schroeijers AB, Izquierdo MA, Wiemer EA, Scheper RJ. Lung resistance-related protein/major vault protein and vaults in multidrug-resistant cancer. Curr Opin Oncol. 2000; 12(6): 550–6. [PubMed: 11085454]
13. Stephen AG, Raval-Fernandes S, Huynh T, Torres M, Kickhoefer VA, Rome LH. Assembly of vault-like particles in insect cells expressing only the major vault protein. J Biol Chem. 2001; 276(26):23217–20. [PubMed: 11349122]
14. van Zon A, Mossink MH, Schoester M, Scheffer GL, Scheper RJ, Sonneveld P, Wiemer EA. Structural domains of vault proteins: a role for the coiled coil domain in vault assembly. Biochem Biophys Res Commun. 2002; 291(3):535–41. [PubMed: 11855821]
15. Kedersha NL, Miquel MC, Bittner D, Rome LH. Vaults. II. Ribonucleoprotein structures are highly conserved among higher and lower eukaryotes. J Cell Biol. 1990; 110(4):895–901. [PubMed: 1691193]
16. Mossink MH, van Zon A, Scheper RJ, Sonneveld P, Wiemer EA. Vaults: a ribonucleoprotein particle involved in drug resistance? Oncogene. 2003; 22(47):7458–67. [PubMed: 14576851]
17. Steiner E, Holzmann K, Elbling L, Micksche M, Berger W. Cellular functions of vaults and their involvement in multidrug resistance. Curr Drug Targets. 2006; 7(8):923–934. [PubMed: 16918321]
18. Izquierdo MA, Scheffer GL, Flens MJ, Giaccone G, Broxterman HJ, Meijer CJ, van der Valk P, Scheper RJ. Broad distribution of the multidrug resistance-related vault lung resistance protein in normal human tissues and tumors. Am J Pathol. 1996; 148(3):877–87. [PubMed: 8774142]
19. Kickhoefer VA, Rajavel KS, Scheffer GL, Dalton WS, Scheper RJ, Rome LH. Vaults are up-regulated in multidrug-resistant cancer cell lines. J Biol Chem. 1998; 273(15):8971–4. [PubMed: 9535882]
20. Izquierdo MA, Shoemaker RH, Flens MJ, Scheffer GL, Wu L, Prather TR, Scheper RJ. Overlapping phenotypes of multidrug resistance among panels of human cancer-cell lines. Int J Cancer. 1996; 65(2):230–7. [PubMed: 8567122]
21. Schroeijers AB, Siva AC, Scheffer GL, de Jong MC, Bolick SC, Dukers DF, Slootstra JW, Meloen RH, Wiemer E, Kickhoefer VA, Rome LH, Scheper RJ. The Mr 193,000 vault protein is up-regulated in multidrug-resistant cancer cell lines. Cancer Res. 2000; 60(4):1104–10. [PubMed: 10706131]
22. Parkin DM, Bray F, Ferlay J, Pisani P. Estimating the world cancer burden: Globocan 2000. Int J Cancer. 2001; 94(2):153–6. [PubMed: 11668491]

23. Umezawa H, Maeda K, Takeuchi T, Okami Y. New antibiotics, bleomycin A and B. J Antibiot. 1966; (19):200–209. [PubMed: 5953301]
24. Einhorn LH. Curing metastatic testicular cancer. Proc Natl Acad Sci U S A. 2002; 99(7):4592–4595. [PubMed: 11904381]
25. Bayer RA, Gaynor ER, Fisher RI. Bleomycin in non-Hodgkin's lymphoma. Semin Oncol. 1992; 19(2 Suppl 5):46–52. discussion 52–3. [PubMed: 1384144]
26. Stubbe J, Kozarich JW. Mechanisms of bleomycin-induced DNA degradation. Chem Rev. 1987; 87(5):1107–1136.
27. Stubbe J, Kozarich JW, Wu W, Vanderwall DE. Bleomycins: A structural model for specificity, binding, and double strand cleavage. Accounts Chem Res. 1996; 29(7):322–330.
28. Chen J, Stubbe J. Bleomycins: towards better therapeutics. Nat Rev Cancer. 2005; 5(2):102–12. [PubMed: 15685195]
29. Cha CH, Saif MW, Yamane BH, Weber SM. Hepatocellular carcinoma: current management. Curr Probl Surg. 2010; 47(1):10–67. [PubMed: 19963083]
30. Nowak AK, Chow PK, Findlay M. Systemic therapy for advanced hepatocellular carcinoma: a review. Eur J Cancer. 2004; 40(10):1474–84. [PubMed: 15196530]
31. Ravry MJ, Omura GA, Bartolucci AA. Phase II evaluation of doxorubicin plus bleomycin in hepatocellular carcinoma: a Southeastern Cancer Study Group trial. Cancer Treat Rep. 1984; 68(12):1517–8. [PubMed: 6210143]
32. Huang CC, Wu MC, Xu GW, Li DZ, Cheng H, Tu ZX, Jiang HQ, Gu JR. Overexpression of the MDR1 gene and P-glycoprotein in human hepatocellular carcinoma. J Natl Cancer Inst. 1992; 84(4):262–4. [PubMed: 1346405]
33. Jones DH, Ley S, Aitken A. Isoforms of 14-3-3 protein can form homo- and heterodimers in vivo and in vitro: implications for function as adapter proteins. FEBS Lett. 1995; 368(1):55–8. [PubMed: 7615088]
34. Tzivion G, Luo Z, Avruch J. A dimeric 14-3-3 protein is an essential cofactor for Raf kinase activity. Nature. 1998; 394(6688):88–92. [PubMed: 9665134]
35. Fu H, Subramanian RR, Masters SC. 14-3-3 proteins: structure, function, and regulation. Annu Rev Pharmacol Toxicol. 2000; 40:617–47. [PubMed: 10836149]
36. Coblitz B, Wu M, Shikano S, Li M. C-terminal binding: an expanded repertoire and function of 14-3-3 proteins. FEBS Lett. 2006; 580(6):1531–5. [PubMed: 16494877]
37. van Heusden GP. 14-3-3 proteins: regulators of numerous eukaryotic proteins. IUBMB Life. 2005; 57(9):623–9. [PubMed: 16203681]
38. van Hemert MJ, Steensma HY, van Heusden GP. 14-3-3 proteins: key regulators of cell division, signalling and apoptosis. Bioessays. 2001; 23(10):936–46. [PubMed: 11598960]
39. Pozuelo Rubio M, Geraghty KM, Wong BH, Wood NT, Campbell DG, Morrice N, Mackintosh C. 14-3-3-affinity purification of over 200 human phosphoproteins reveals new links to regulation of cellular metabolism, proliferation and trafficking. Biochem J. 2004; 379(Pt 2):395–408. [PubMed: 14744259]
40. Meek SE, Lane WS, Piwnica-Worms H. Comprehensive proteomic analysis of interphase and mitotic 14-3-3-binding proteins. J Biol Chem. 2004; 279(31):32046–54. [PubMed: 15161933]
41. Jin J, Smith FD, Stark C, Wells CD, Fawcett JP, Kulkarni S, Metalnikov P, O'Donnell P, Taylor P, Taylor L, Zougman A, Woodgett JR, Langeberg LK, Scott JD, Pawson T. Proteomic, functional, and domain-based analysis of in vivo 14-3-3 binding proteins involved in cytoskeletal regulation and cellular organization. Curr Biol. 2004; 14(16):1436–50. [PubMed: 15324660]
42. Benzinger A, Muster N, Koch HB, Yates JR 3rd, Hermeking H. Targeted proteomic analysis of 14-3-3 sigma, a p53 effector commonly silenced in cancer. Mol Cell Proteomics. 2005; 4(6):785–95. [PubMed: 15778465]
43. Aitken A. Functional specificity in 14-3-3 isoform interactions through dimer formation and phosphorylation. Chromosome location of mammalian isoforms and variants. Plant Mol Biol. 2002; 50(6):993–1010. [PubMed: 12516867]
44. Seow TK, Ong SE, Liang RC, Ren EC, Chan L, Ou K, Chung MC. Two-dimensional electrophoresis map of the human hepatocellular carcinoma cell line, HCC-M, and identification

of the separated proteins by mass spectrometry. Electrophoresis. 2000; 21(9):1787–1813. [PubMed: 10870966]

45. Lee CL, Hsiao HH, Lin CW, Wu SP, Huang SY, Wu CY, Wang AH, Khoo KH. Strategic shotgun proteomics approach for efficient construction of an expression map of targeted protein families in hepatoma cell lines. Proteomics. 2003; 3(12):2472–86. [PubMed: 14673797]
46. Ko BS, Chang TC, Hsu C, Chen YC, Shen TL, Chen SC, Wang J, Wu KK, Jan YJ, Liou JY. Overexpression of 14-3-3epsilon predicts tumour metastasis and poor survival in hepatocellular carcinoma. Histopathology. 2011; 58(5):705–11. [PubMed: 21401702]
47. Yang X, Zou P, Yao J, Yun D, Bao H, Du R, Long J, Chen X. Proteomic dissection of cell type-specific H2AX-interacting protein complex associated with hepatocellular carcinoma. J Proteome Res. 2010; 9(3):1402–15. [PubMed: 20000738]
48. Pear WS, Nolan GP, Scott ML, Baltimore D. Production of high-titer helper-free retroviruses by transient transfection. Proc Natl Acad Sci U S A. 1993; 90(18):8392–6. [PubMed: 7690960]
49. Chen TR. Re-evaluation of HeLa, HeLa S3, and HEp-2 karyotypes. Cytogenet Cell Genet. 1988; 48(1):19–24. [PubMed: 3180844]
50. Lou Z, Minter-Dykhouse K, Franco S, Gostissa M, Rivera MA, Celeste A, Manis JP, van Deursen J, Nussenzweig A, Paull TT, Alt FW, Chen J. MDC1 maintains genomic stability by participating in the amplification of ATM-dependent DNA damage signals. Mol Cell. 2006; 21(2):187–200. [PubMed: 16427009]
51. Shevchenko A, Tomas H, Havlis J, Olsen JV, Mann M. In-gel digestion for mass spectrometric characterization of proteins and proteomes. Nat Protoc. 2006; 1(6):2856–60. [PubMed: 17406544]
52. Minaguchi T, Waite KA, Eng C. Nuclear localization of PTEN is regulated by Ca(2+) through a tyrosil phosphorylation-independent conformational modification in major vault protein. Cancer Res. 2006; 66(24):11677–82. [PubMed: 17178862]
53. Fernandes-Alnemri T, Litwack G, Alnemri ES. CPP32, a novel human apoptotic protein with homology to Caenorhabditis elegans cell death protein Ced-3 and mammalian interleukin-1 beta-converting enzyme. J Biol Chem. 1994; 269(49):30761–4. [PubMed: 7983002]
54. Nicholson DW, Ali A, Thornberry NA, Vaillancourt JP, Ding CK, Gallant M, Gareau Y, Griffin PR, Labelle M, Lazebnik YA. Identification and inhibition of the ICE/CED-3 protease necessary for mammalian apoptosis. Nature. 1995; 376(6535):37–43. [PubMed: 7596430]
55. Oliver FJ, de la Rubia G, Rolli V, Ruiz-Ruiz MC, de Murcia G, Murcia JM. Importance of poly(ADP-ribose) polymerase and its cleavage in apoptosis. Lesson from an uncleavable mutant. J Biol Chem. 1998; 273(50):33533–9. [PubMed: 9837934]
56. Fillingham J, Keogh M-C, Krogan NJ. gamma H2AX and its role in DNA double-strand break repair. Biochem Cell Bio. 2006; 84(4):568–577. [PubMed: 16936829]
57. Chen Y, Poon RYC. The multiple checkpoint functions of CHK1 and CHK2 in maintenance of genome stability. Front Biosci. 2008; 13:5016–5029. [PubMed: 18508566]
58. Rome L, Kedersha N, Chugani D. Unlocking vaults: organelles in search of a function. Trends Cell Biol. 1991; 1(2–3):47–50. [PubMed: 14731565]
59. Tzivion G, Gupta VS, Kaplun L, Balan V. 14-3-3 proteins as potential oncogenes. Semin Cancer Biol. 2006; 16(3):203–213. [PubMed: 16725345]
60. Telles E, Hosing AS, Kundu ST, Venkatraman P, Dalal SN. A novel pocket in 14-3-3epsilon is required to mediate specific complex formation with cdc25C and to inhibit cell cycle progression upon activation of checkpoint pathways. Exp Cell Res. 2009; 315(8):1448–57. [PubMed: 19331823]
61. Dalal SN, Yaffe MB, DeCaprio JA. 14-3-3 family members act coordinately to regulate mitotic progression. Cell Cycle. 2004; 3(5):672–7. [PubMed: 15107609]
62. Stavridi ES, Chehab NH, Malikzay A, Halazonetis TD. Substitutions that compromise the ionizing radiation-induced association of p53 with 14-3-3 proteins also compromise the ability of p53 to induce cell cycle arrest. Cancer Res. 2001; 61(19):7030–3. [PubMed: 11585729]
63. Kickhoefer VA, Poderycki MJ, Chan EK, Rome LH. The La RNA-binding protein interacts with the vault RNA and is a vault-associated protein. J Biol Chem. 2002; 277(43):41282–6. [PubMed: 12196535]

64. Zheng CL, Sumizawa T, Che XF, Tsuyama S, Furukawa T, Haraguchi M, Gao H, Gotanda T, Jueng HC, Murata F, Akiyama S. Characterization of MVP and VPARP assembly into vault ribonucleoprotein complexes. Biochem Biophys Res Commun. 2005; 326(1):100–7. [PubMed: 15567158]
65. van Zon A, Mossink MH, Schoester M, Houtsmuller AB, Scheffer GL, Scheper RJ, Sonneveld P, Wiemer EA. The formation of vault-tubes: a dynamic interaction between vaults and vault PARP. J Cell Sci. 2003; 116(Pt 21):4391–400. [PubMed: 13130096]
66. Yaffe MB, Rittinger K, Volinia S, Caron PR, Aitken A, Leffers H, Gamblin SJ, Smerdon SJ, Cantley LC. The structural basis for 14-3-3:phosphopeptide binding specificity. Cell. 1997; 91(7): 961–71. [PubMed: 9428519]
67. Herrmann C, Kellner R, Volknandt W. Major vault protein of electric ray is a phosphoprotein. Neurochem Res. 1998; 23(1):39–46. [PubMed: 9482265]
68. Ehrnsperger C, Volknandt W. Major vault protein is a substrate of endogenous protein kinases in CHO and PC12 cells. Biol Chem. 2001; 382(10):1463–71. [PubMed: 11727830]
69. Kolli S, Zito CI, Mossink MH, Wiemer EAC, Bennett AM. The Major Vault Protein Is a Novel Substrate for the Tyrosine Phosphatase SHP-2 and Scaffold Protein in Epidermal Growth Factor Signaling. J Biol Chem. 2004; 279(28):29374–29385. [PubMed: 15133037]
70. Yuan L, Yu WM, Qu CK. DNA damage-induced G2/M checkpoint in SV40 large T antigen-immortalized embryonic fibroblast cells requires SHP-2 tyrosine phosphatase. J Biol Chem. 2003; 278(44):42812–20. [PubMed: 12937170]
71. Seimiya H, Sawada H, Muramatsu Y, Shimizu M, Ohko K, Yamane K, Tsuruo T. Involvement of 14-3-3 proteins in nuclear localization of telomerase. EMBO J. 2000; 19(11):2652–61. [PubMed: 10835362]
72. Tanaka H, Kato K, Yamashita E, Sumizawa T, Zhou Y, Yao M, Iwasaki K, Yoshimura M, Tsukihara T. The structure of rat liver vault at 3.5 angstrom resolution. Science. 2009; 323(5912): 384–8. [PubMed: 19150846]
73. Morrison DK. The 14-3-3 proteins: integrators of diverse signaling cues that impact cell fate and cancer development. Trends Cell Biol. 2009; 19(1):16–23. [PubMed: 19027299]
74. Wilker E, Yaffe MB. 14-3-3 Proteins--a focus on cancer and human disease. J Mol Cell Cardiol. 2004; 37(3):633–42. [PubMed: 15350836]
75. Hermeking H. The 14-3-3 cancer connection. Nat Rev Cancer. 2003; 3(12):931–943. [PubMed: 14737123]
76. Moritz A, Li Y, Guo A, Villen J, Wang Y, MacNeill J, Kornhauser J, Sprott K, Zhou J, Possemato A, Ren JM, Hornbeck P, Cantley LC, Gygi SP, Rush J, Comb MJ. Akt-RSK-S6 kinase signaling networks activated by oncogenic receptor tyrosine kinases. Sci Signal. 2010; 3(136):ra64. [PubMed: 20736484]
77. Gu TL, Deng X, Huang F, Tucker M, Crosby K, Rimkunas V, Wang Y, Deng G, Zhu L, Tan Z, Hu Y, Wu C, Nardone J, MacNeill J, Ren J, Reeves C, Innocenti G, Norris B, Yuan J, Yu J, Haack H, Shen B, Peng C, Li H, Zhou X, Liu X, Rush J, Comb MJ. Survey of tyrosine kinase signaling reveals ROS kinase fusions in human cholangiocarcinoma. PLoS ONE. 2011; 6(1):e15640. [PubMed: 21253578]
78. Gu TL, Cherry J, Tucker M, Wu J, Reeves C, Polakiewicz RD. Identification of activated Tnk1 kinase in Hodgkin's lymphoma. Leukemia. 2010; 24(4):861–5. [PubMed: 20090780]
79. Rikova K, Guo A, Zeng Q, Possemato A, Yu J, Haack H, Nardone J, Lee K, Reeves C, Li Y, Hu Y, Tan Z, Stokes M, Sullivan L, Mitchell J, Wetzel R, Macneill J, Ren JM, Yuan J, Bakalarski CE, Villen J, Kornhauser JM, Smith B, Li D, Zhou X, Gygi SP, Gu TL, Polakiewicz RD, Rush J, Comb MJ. Global survey of phosphotyrosine signaling identifies oncogenic kinases in lung cancer. Cell. 2007; 131(6):1190–203. [PubMed: 18083107]
80. Thingholm TE, Larsen MR, Ingrell CR, Kassem M, Jensen ON. TiO(2)-based phosphoproteomic analysis of the plasma membrane and the effects of phosphatase inhibitor treatment. J Proteome Res. 2008; 7(8):3304–13. [PubMed: 18578522]
81. Olsen JV, Vermeulen M, Santamaria A, Kumar C, Miller ML, Jensen LJ, Gnad F, Cox J, Jensen TS, Nigg EA, Brunak S, Mann M. Quantitative phosphoproteomics reveals widespread full phosphorylation site occupancy during mitosis. Sci Signal. 2010; 3(104):ra3. [PubMed: 20068231]

82. Ruse CI, McClatchy DB, Lu B, Cociorva D, Motoyama A, Park SK, Yates JR 3rd. Motif-specific sampling of phosphoproteomes. J Proteome Res. 2008; 7(5):2140–50. [PubMed: 18452278]

83. Han G, Ye M, Liu H, Song C, Sun D, Wu Y, Jiang X, Chen R, Wang C, Wang L, Zou H. Phosphoproteome analysis of human liver tissue by long-gradient nanoflow LC coupled with multiple stage MS analysis. Electrophoresis. 2010; 31(6):1080–9. [PubMed: 20166139]

84. Dephoure N, Zhou C, Villen J, Beausoleil SA, Bakalarski CE, Elledge SJ, Gygi SP. A quantitative atlas of mitotic phosphorylation. Proc Natl Acad Sci U S A. 2008; 105(31):10762–7. [PubMed: 18669648]

Synopsis

In response to BLM treatment, 14-3-3 dimer, in a phosphorylation-dependent manner, binds to MVP monomers. The binding may interfere with MVP-directed vault assembly, leading to reduce the numbers of intact functional vault particle for subsequent BLM extrusion, thereby resulting in more BLM molecules accumulated at their targets to increase DNA damage and consequently elevate the cellular DNA damage response (DDR) in cells.

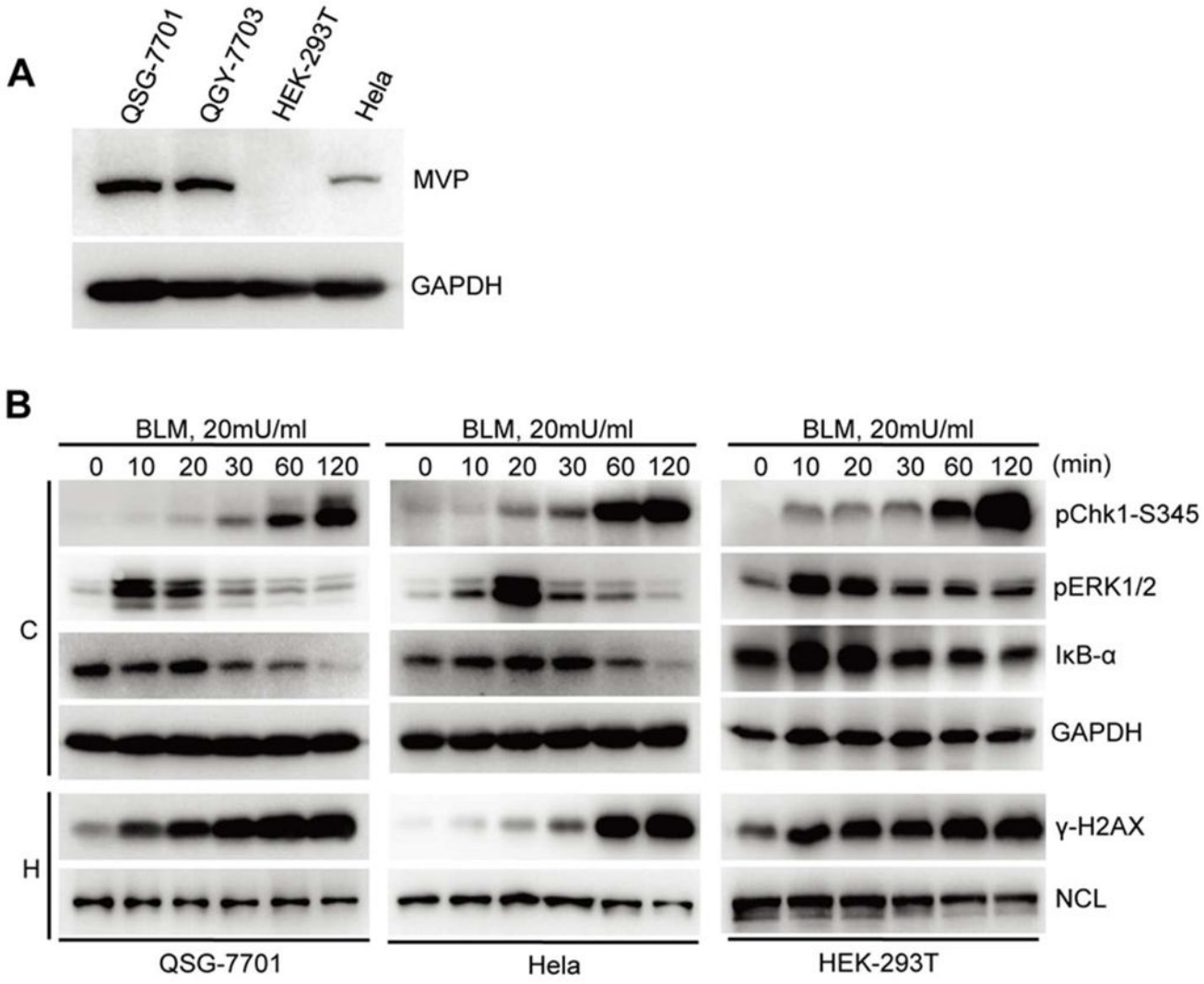

Figure 1.

Time-dependent changes of cellular DDR to BLM in different cell lines. **(A)** Immunoblotting analysis of MVP expression levels in different cell lines. **(B)** Immunoblotting analysis of time-dependent changes of cellular DDR to BLM in different cell lines. QSG-7701: hepatocyte; QGY-7703: HCC cell; HEK-293T: human embryonic kidney cell; Hela: human cervical carcinoma cell.

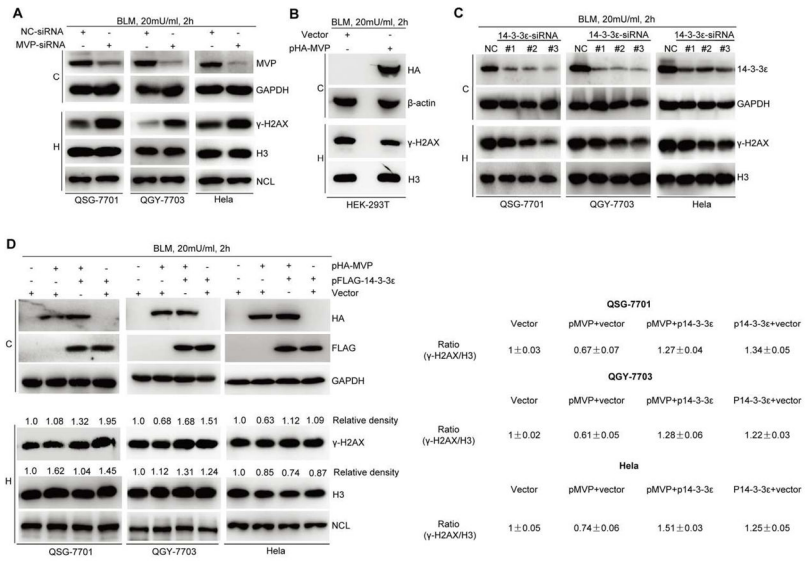

Figure 2.

MVP possesses the specific activity to resist BLM-induced DDR while 14-3-3ε interacts with MVP to enhance the cellular DDR to BLM. **(A)** Knock-down of MVP results in remarkable elevation of cellular DDR to BLM in all tested cell lines, indicating that MVP indeed possesses the drug resistance activity. **(B)** Exogenous expression of MVP in MVP-negative cell line-HEK-293T also leads to resist BLM-induced DDR. **(C)** Knock-down of 14-3-3ε leads to a general decrease of BLM-induced DDR in all tested cell lines, indicating that 14-3-3ε promotes cellular DDR to BLM. **(D)** 14-3-3ε inhibits MVP to enhance BLM-induced DDR. The band density on the blots was measured by using the analysis tool mounted on FuJiFilm Las3000 instrument (FuJiFilm, Japan) where the blots were exposed. After the measurement, the densities of γ-H2AX and H3 in control cells (vector) were set as 1.0, respectively. The densities of the other bands were correspondingly normalized. Then the ratios (γ-H2AX/H3) were calculated for comparing the changes among samples. C: Cytoplasmic fraction. GAPDH was used as the loading control for the cytoplasmic fractions; H: HCl-extracted histone fraction. H3 and NCL were used as the loading control for γ-H2AX (histone fractions).

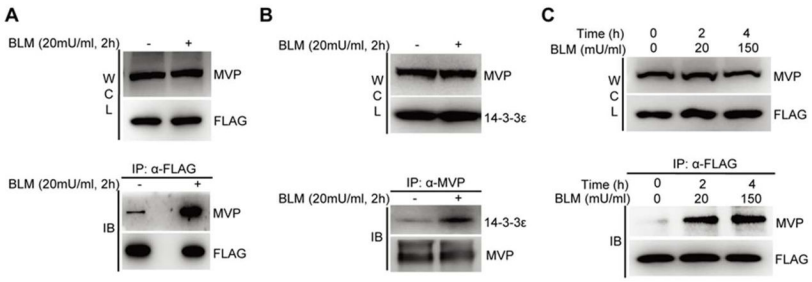

Figure 3.

MVP is BLM-inducible 14-3-3ε interactor in HCC cells. **(A)** Immunoblotting analysis of BLM-induced interaction between 14-3-3ε and MVP in stable FLAG-14-3-3ε expressing HCC cells. **(B)** Immunoblotting analysis of BLM-induced interaction between 14-3-3ε and MVP in parental HCC cells. **(C)** Immunoblotting analysis of the BLM-induced time- and dose-dependent interaction between 14-3-3ε and MVP. WCL: whole cell lysates; IP: immunoprecipitation; IB: immunoblotting.

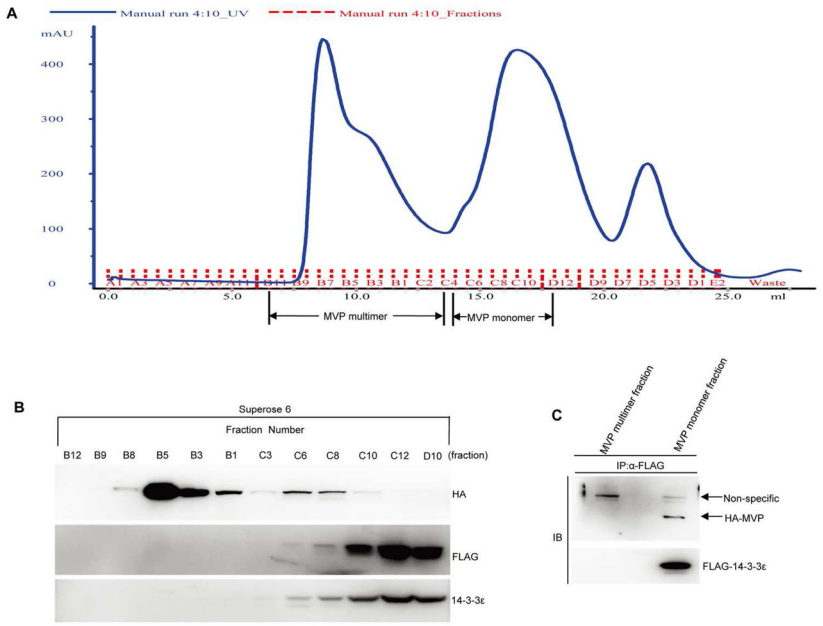

Figure 4.

14-3-3ε associates with MVP monomer in response to BLM treatment. **(A)** The elution profile of cell extracts derived from HEK-293T cells co-transfected with HA-tagged MVP and FLAG-tagged 14-3-3ε on Superose 6 10/300 GL column. **(B)** Immunoblotting analysis of the distribution of MVP multimer, MVP monomer and 14-3-3ε. **(C)** 14-3-3ε associates with MVP monomer. The fractions containing either multimerized or monomer MVP were combined respectively to perform immunoprecipitation using anti-FLAG beads. IP: immunoprecipitation; IB: immunoblotting.

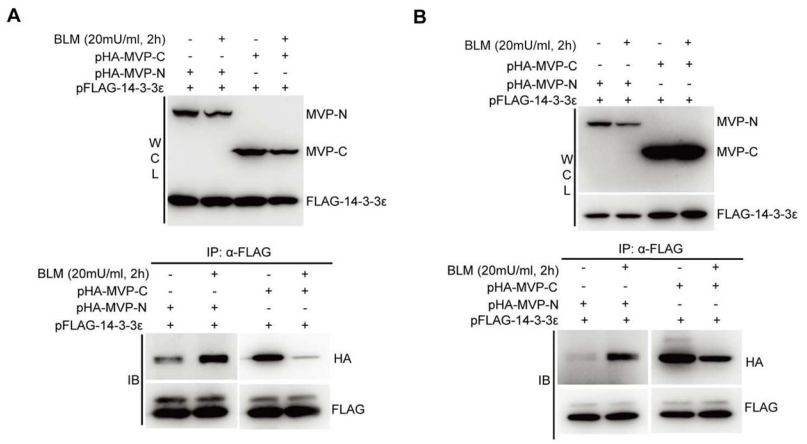

Figure 5.

Both MVP N- and C-terminal domains are involved in mediating 14-3-3ε binding in response to BLM treatment. A: in HEL-293T cells. B: in HCC cells. WCL: whole cell lysates; IP: immunoprecipitation; IB: immunoblotting.

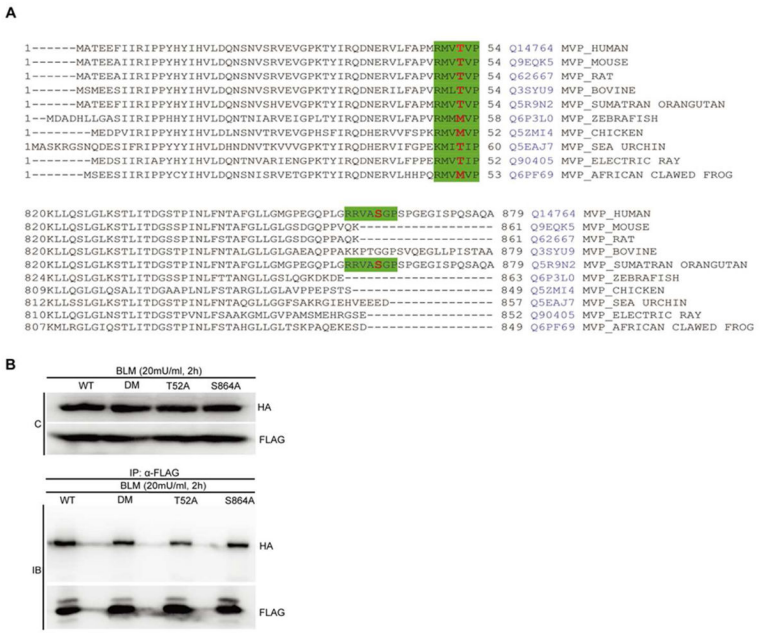

Figure 6.

14-3-3ε binds to MVP in a phosphorylation-dependent manner in response to BLM treatment. **(A)** Sequence alignment analysis of the putative 14-3-3 binding motifs on MVP. In human MVP, R49-P54 and R860-P866 are the two putative 14-3-3 binding motifs on MVP. The T52 and S864 residues marked in red are putative phosphorylation sites, respectively. **(B)** BLM triggers the phosphorylation of T52 on MVP, which together with the phosphorylated S864 mediates 14-3-3ε binding. DM: double-mutant MVP (T52A/S864A); IP: immunoprecipitation; IB: immunoblotting.

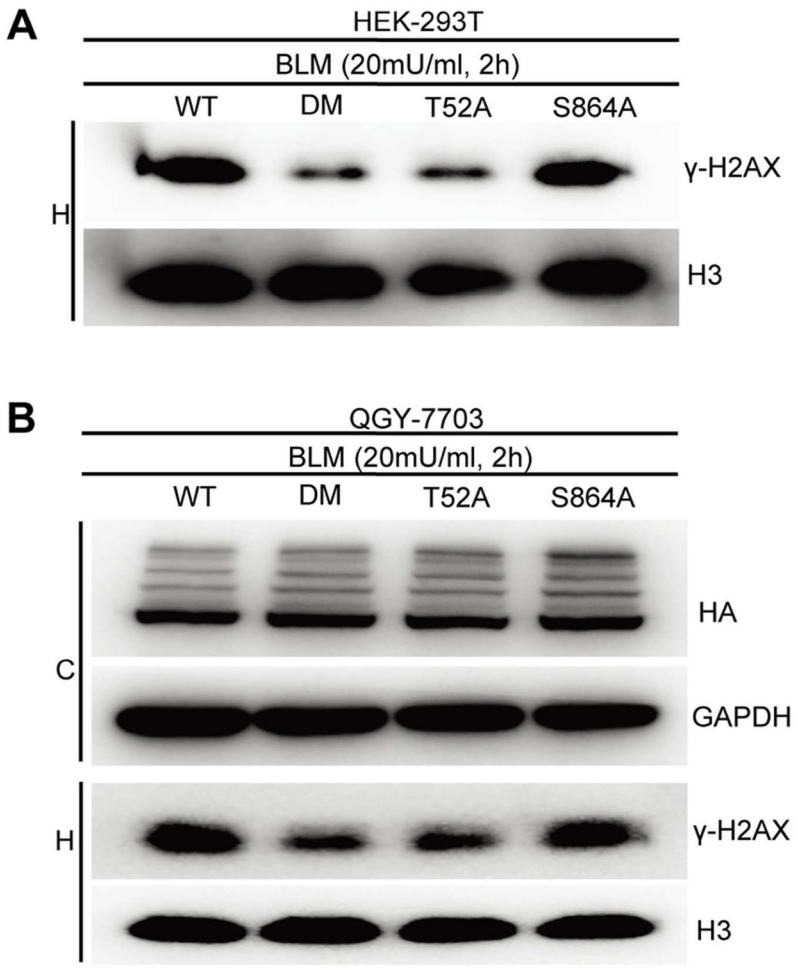

Figure 7.

MVP mutants exert more drug resistance activity to BLM. Either wild-type (WT) MVP or the site-specific MVP mutants (T52A, S864A and T52A/S864A (DM)) was individually transfected into HEK-293T cell and HCC cell, respectively. Subcellular fractions were extracted after BLM treatment and analyzed with the indicated antibodies by immunoblotting. A: In HEK-293T cells, the cytoplasmic fractions are shown in Figure 6B; B: In HCC cells. C: Cytoplasmic fraction. GAPDH was used as the loading control for the cytoplasmic fractions; H: HCl-extracted histone fraction. H3 was used as the loading control for γ-H2AX (histone fractions).

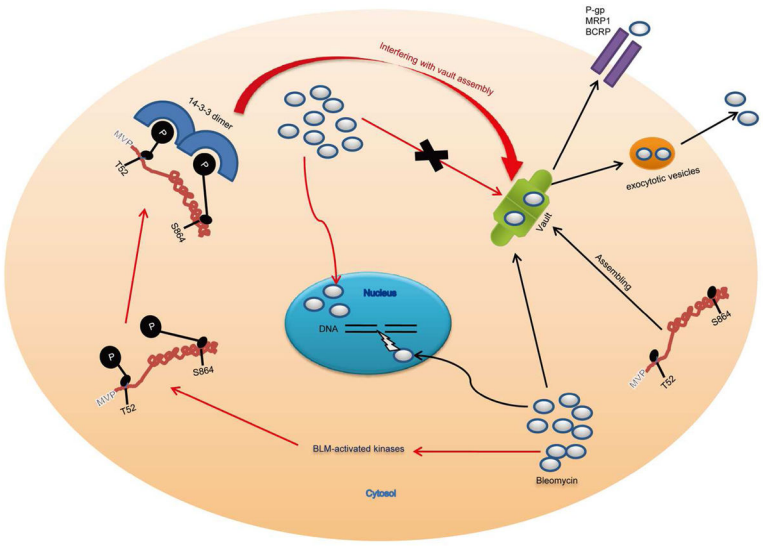

Figure 8.

Proposed mechanism for 14-3-3ε interfering with MVP-mediated vault assembly to increase BLM-induced DNA damage. Previous model proposed that MVP-assembled vault particles can compartmentalize drugs into their hollow cavity, and through coordinating with exocytotic vesicles or efflux pumps such as P-gp, MRP1 and breast resistance protein (BCRP) to extrude drugs from the cells(indicated by black arrows)[16]. Here, we propose that 14-3-3 dimer, in a phosphorylation-dependent manner, binds to MVP monomer. The binding may interfere with MVP-mediated vault assembly or inhibit the exchange between MVP monomer and vault-mounted MVP molecule, which leads to reduce the numbers of intact functional vault particles for the subsequent BLM extrusion, thereby, resulting in increase of BLM molecules accumulated at their targets followed by DNA damage and elevated cellular DDR(indicated by red arrows).

Table 1

Summary of the peptides sequenced for 14-3-3ε and MVP respectively by LC-MS/MS.

Protein name	Peptide sequence	MH+	z	Score
14-3-3 protein epsilon (IPI00000816.1)[a]	R.YDEMVESMK.K	1131.46967	2	2.62
	K.EALQDVEDENQ.-	1289.54918	2	2.70
	K.EAAENSLVAYK.A	1194.60009	2	2.81
	R.YLAEFATGNDR.K	1256.59059	2	3.69
	K.AASDIAM*TELPPTHPIR.L	1838.95081	3	3.96
	K.VAGMDVELTVEER.N	1450.72852	2	3.68
	R.DNLTLWTSDMQGDGEEQNK.E	2180.94007	2	5.87
	R.NLLSVAYKNVIGAR.R	1517.87984	2	3.27
	K.DSTLIMQLLR.D	1198.71732	2	3.02
	K.AAFDDAIAELDTLSEESYK.D	2094.00314	2	5.88
major vault protein (MVP) (IPI00000105.4)[a]	K.AQQLAEVEVK.K	1117.62906	2	3.32
	R.ALQPLEEGEDEEK.V	1486.69076	2	2.98
	R.VPHNAAVQVYDYR.E	1531.76520	2	2.95
	R.DLAVAGPEMQVK.L	1260.66955	2	3.12
	K.ALLDFEDK.D	956.52054	2	2.80
	K.AQALAIETEAELQR.V	1548.84981	2	4.29
	R.GAVASVTFDDFHK.N	1393.67466	2	3.79
	R.VASGPSPGEGISPQSAQAPQAPGDNHVVPVLR.-	3122.60565	3	5.26
	R.TAVFGFETSEAK.G	1286.62631	2	3.15
	K.VSHQAGDHWLIR.G	1421.74756	2	2.75
	R.IPPYHYIHVLDQNSNVSR.V	2155.11221	2	5.11
	R.SVQLAIEITTNSQEAAAK.H	1877.00535	2	3.97
	R.QAIPLDENEGIYVQDVK.T	1933.99445	2	3.93
	R.LAQDPFPLYPGEVLEK.D	1815.95273	2	2.90
	R.DQAVFPQNGLVVSSVDVQSVEPVDQR.T	2815.42998	2	4.38
	R.DAQGLVLFDVTGQVR.L	1617.85950	2	4.37
	R.AVIGSTYMLTQDEVLWEK.E	2083.04162	2	4.23
	K.VVAGDEWLFEGPGTYIPR.K	2009.02060	2	4.87
	R.KELLELEALSMAVESTGTAK.A	2132.19071	2	4.27
	K.ELLELEALSMAVESTGTAK.A	2004.09575	2	5.27
	R.KEVEVVEIIQATIIR.Q	1740.02656	2	5.55
	R.VVFGPELVSLGPEEQFTVLSLSAGR.P	2643.47804	2	4.71

[a]Protein accession number. M* represents the oxidized Met residue.